DEVELOPMENTAL DYNAMICS 219:391–401 (2000)

Modulation of Cell Proliferation in the Embryonic Retina of Zebrafish (*Danio rerio*)

ZHENG LI, MINJIE HU, MALGORZATA J. OCHOCINSKA, NANCY M. JOSEPH, AND STEPHEN S. EASTER JR.*

Department of Biology, University of Michigan, Ann Arbor, Michigan

ABSTRACT **We describe light-microscopically the development of the embryonic zebrafish eye with particular attention to cell number, cell proliferation, and cell death. The period from 16 to 36 hr post fertilization (hpf) comprises two phases; during the first (16–27 hpf) the optic vesicle becomes the eye cup, and during the second (27–36 hpf) the eye cup begins to differentiate into the neural retina and pigmented epithelium. All cells in the eye primordium are proliferative prior to 28 hpf, and the length of the cell cycle has been estimated to be 10 hr at 24–28 hpf (Nawrocki, 1985). Our cell counts are consistent with that estimate at that age, but not at earlier ages. A 10-hr cell cycle predicts that the cell number should increase by 7% per hr, but during 16–24 hpf the cell number increased by only 1.5% per hr. Despite the low rate of increase, all cells labeled with bromo-deoxyuridine, so all were proliferative. We considered three possible explanations for the nearly-constant cell number in the first phase: proliferation balanced by cell emigration from the eye, proliferation balanced by cell death, and low proliferation caused by a transient prolongation of the cell cycle. We excluded the first two, and found direct support for the third. Previous examinations of the cell cycle length in vertebrate central nervous system have concluded that it increases monotonically, in contrast to the modulation that we have shown. Modulation of the cell cycle length is well-known in flies, but it is generally effected by a prolonged arrest at one phase, in contrast to the general deceleration that we have shown.** **© 2000 Wiley-Liss, Inc.**

Key words: apoptosis; cell cycle; cell death; growth; morphogenesis; optic vesicle; pigmented epithelium; proliferation; retina; zebrafish

INTRODUCTION

The zebrafish optic vesicle develops into the eye cup over about 11 hr, from 16 to 27 hr post fertilization (hpf) (Kimmel et al., 1995; Schmitt and Dowling, 1994), during which time all cells are proliferative. The first terminal divisions occur at about 28 hpf (Hu and Easter, 1999; Nawrocki, 1985) and neurogenesis continues thereafter throughout much of the fish's life (Marcus et al., 1999). The vesicle is flat, and its two layers are nearly equal in thickness. The eye cup is round, with the lateral layer (LL) having become the neural retina (NR) and the medial layer (ML) having become the pigmented epithelium (PE). Cells move from the ML to the LL, and this cellular rearrangement contributes to the simultaneous thickening of the LL/NR and thinning of the ML/PE (Li et al., 2000). In spite of the radical changes in the shape and in the relative volumes of the two layers, their combined volumes remained nearly constant throughout morphogenesis (Li et al., 2000).

The volume could be maintained constant by four mechanisms, alone or in combination: a low rate of cell proliferation, proliferation accompanied by a high rate of cell death, volume-conservative cytokinesis (as commonly occurs during cleavage stages), and proliferation balanced by cell emigration from the vesicle. Cell emigration is the only one of them that can presently be excluded, because our fate map of the optic vesicle provided no evidence for it (Li et al., 2000). Indeed, some slight *im*migration from the optic stalk into the vesicle may have occurred (Holt, 1980). To our knowledge, none of the other three mechanisms have been examined in detail during the morphogenesis of any tissue. Cleavage-like cytokinesis, in which the volume of the daughter cells together equals that of the mother cell, has been proposed to account for the roughly constant volume of the developing amphibian neural plate (Gillette, 1944), but this hypothesis was not tested further. Cell death in the central nervous system (CNS) is often quite significant after the neurons have formed and their axons have reached their targets (reviewed by Oppenheim, 1991). But during the period before neurogenesis, the period that concerns us in the eye, cell death is generally less common. Slow prolifer-

Grant sponsor: National Eye Institute; Grant number: R01-EY00168.

Dr. Zheng Li's present address is Pfizer Global Research and Development, Ann Arbor Laboratories, 2800 Plymouth Road, Ann Arbor, MI 48105.

Dr. Minjie Hu's present address is Arbor Vita Corporation, 772 Lucerne Drive, Sunnyvale, CA 94086.

*Correspondence to: Prof. S.S. Easter, Jr., Department of Biology, University of Michigan, 830 N. University Avenue, Ann Arbor, MI 48109-1048. E-mail: sseaster@umich.edu

Received 10 July 2000; Accepted 4 August 2000

ation has been suggested to accompany morphogenesis because mitotic figures were sparse during the shaping of the neural plate and more numerous afterward (Burnside and Jacobson, 1968; Burt, 1943). But these observations were not pursued more rigorously, e.g., by counting cells.

We have evaluated these three possibilities independently, and we conclude that the rate of proliferation transiently decreases during morphogenesis and then increases thereafter. The slowing results from an increase in the duration of the cell cycle (T_C) in all cells, rather than the withdrawal of some cells from the cycle. T_C decreases again, and proliferation increases, following the formation of the eye cup. This up-and-down modulation of T_C is a novel result, as previous work on proliferation in the vertebrate CNS has emphasized the monotonic *increase* of T_C with embryonic age (reviewed by Alexiades and Cepko, 1996; Caviness et al., 2000; Jacobson, 1991). Some of these results have been presented previously in abstract form (Li and Easter, 1997).

RESULTS

Cell Numbers

The rate of proliferation (the number of new cells produced per hr) is governed by the fraction of cells that are proliferative and by T_C. Initially all cells are proliferative, but as some withdraw from the cycle those that remain generally adopt a longer T_C (Alexiades and Cepko, 1996; Caviness et al., 2000; Jacobson, 1991). In the presumptive NR the entire population of cells is proliferative prior to 28 hpf (Hu and Easter, 1999; Nawrocki, 1985), and at 24 hpf T_C is about 10 hr (Nawrocki, 1985), so conventional wisdom would predict that the cell cycle prior to 24 hpf would be 10 hr or less. If T_C were 10 hr then the fractional increase per hr would be:

$$2^{(1/10)} - 1 = 0.07$$

or 7%. During the 11 hr (16–27 hpf) of eye cup formation, then the number of cells should increase by 114%, and if T_C were less, then cell number should have increased by even more. Such a large increase in cell number in a tissue of constant volume would indicate that cytokinesis must have been volume-conservative. Alternatively, if the cell number did not increase as predicted, then cell proliferation may have transiently decreased or cell death increased or both, and these alternatives could be checked independently. For these reasons, we counted cells.

Figure 1A shows the number of cells in the eye as a function of age, 16–36 hpf. (Prior to 16 hpf, the boundary between the optic vesicle and the neural tube is unclear (Schmitt and Dowling, 1994) so numbers cannot be computed.) At 16 hpf the numbers of cells were nearly equal on the two sides (665 ± 26 on the LL/NR and 587 ± 27 on the ML/PE), but by 27 hpf, the LL/NR

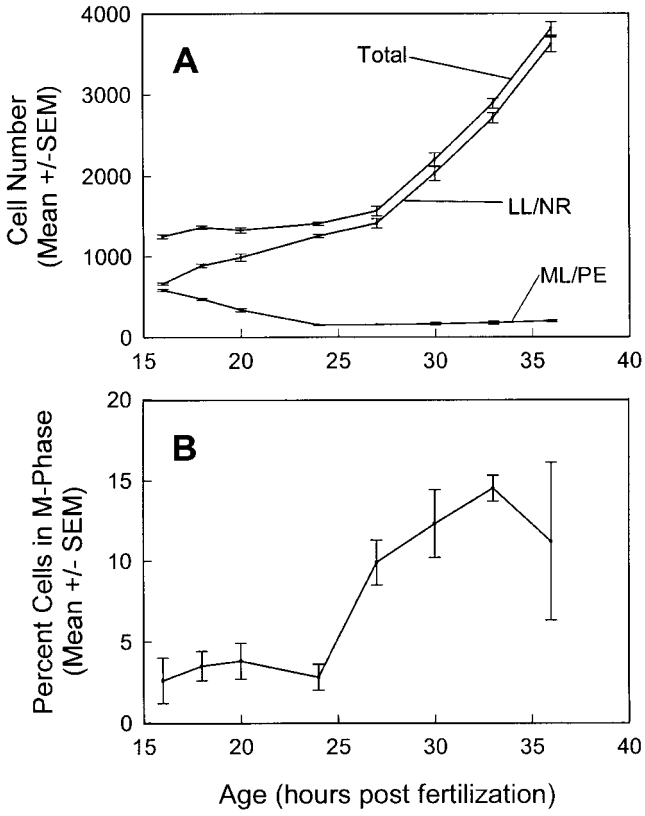

Fig. 1. Changes in the numbers of cells and mitotic figures as a function of age. Means ± SEM, N = 4 at all points. **A**: Number of cells, including interphase, mitotic, and pyknotic. The lower points indicate those in the medial layer/pigmented epithelium (ML/PE), the middle points are those in the lateral layer/neural retina (LL/NR), and the upper points are the sum of the two (Total). **B**: Percentage of cells in M-phase. Raw numbers were obtained from the same sections that produced Figure 1A, and percentages were computed relative to those totals. The mitotic figures appeared in both layers initially, but after about 20 hpf nearly all were in the LL/NR.

had increased by 745 cells (to 1410 ± 58) as the ML/PE had decreased by 432 cells (to 155 ± 3). The total number of cells in both layers increased by 313 cells (from 1252 ± 49 to 1565 ± 56), or 25%. The loss from the ML/PE and the gain in the LL/NR support the idea that cell rearrangement accounted for most of the increase in numerical disparity between the two layers (Li et al., 2000), but a little proliferation, enough to produce 313 cells, was also required. A 114% increase in cell number, to be expected from a 10 hr T_C over an 11-hr interval, is 1427 new cells. The fact that the number increased by only 313, 1114 less than predicted, implies that either proliferation was less than expected or it was balanced by the death of about 1114 cells.

Cell Death

Cell death was evaluated quantitatively by scoring pyknotic cells. In sections, they were so few that it was impossible to estimate their numbers reliably with our

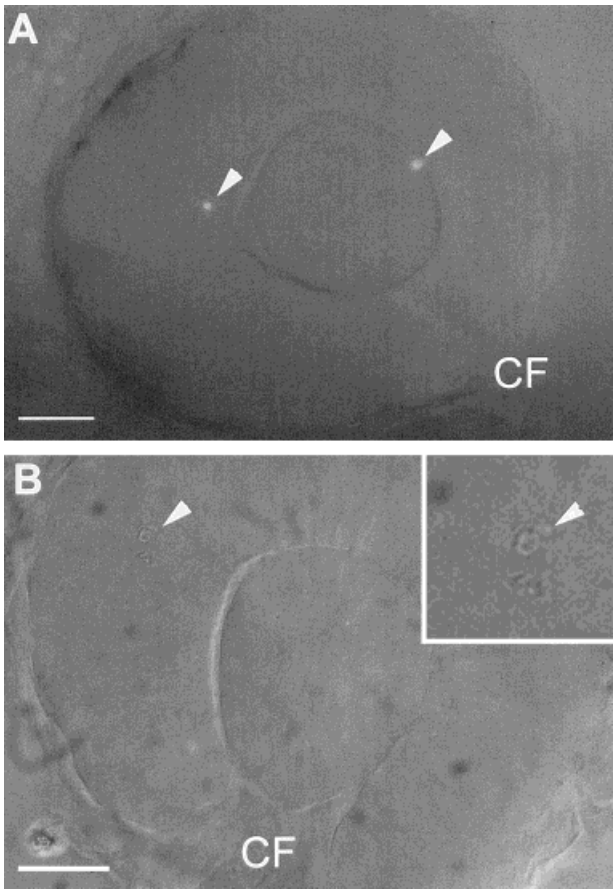

Fig. 2. Dying cells seen in photomicrographs of live eyes in situ in 22 hpf embryos. **A**: Fluorescence viewing. The bright spots (arrowheads) are acridine orange-positive (AO+) cells, labeled by immersion of the embryo for 1 hr in a 1% solution of AO. The one on the left is in the neural retina, the one on the right, in the lens. **B**: Differential interference contrast viewing. A pyknotic nucleus (arrowhead) is identified by its globular/refractile character, and is shown at higher magnification in the inset. Scale bars = 20 μm. CF, choroid fissure.

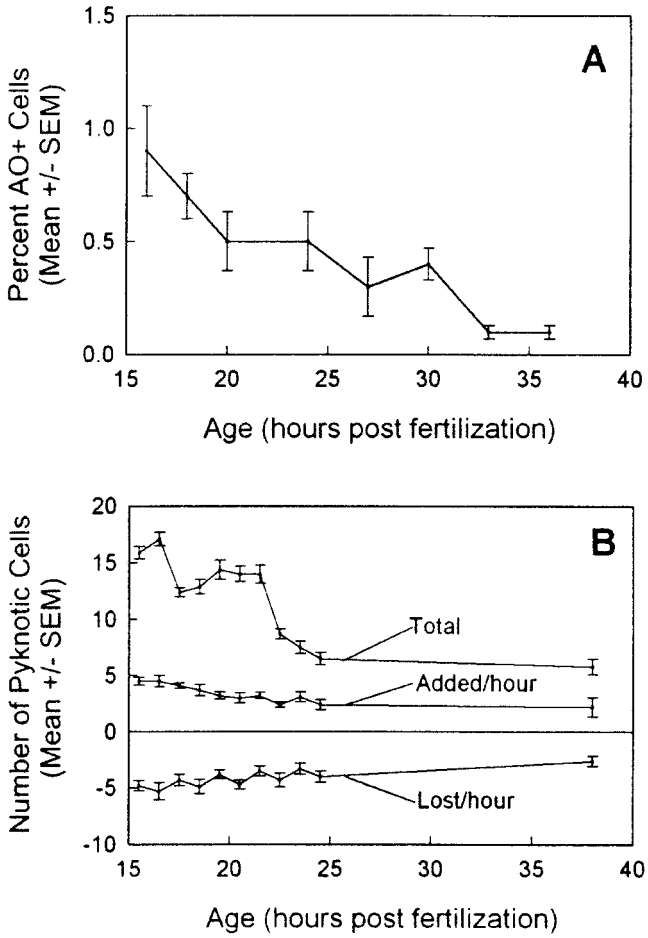

Fig. 3. Dying cells as a function of age. Means ± SEM. **A**: The percentage of cells in the eye that were AO+ immediately following a 1-hr immersion in 1% AO. The cells were counted and the percentages were calculated from the data in Figure 1A. N≥3 at all points. **B**: The appearance and disappearance of pyknotic cells (globular/refractile criterion) in the eyes of living embryos. The uppermost points show the number present at particular times; they represent single "snapshots"—views of the number of dying cells at particular times. In contrast, the lower two sets of points show rates of appearance and disappearance of pyknotic cells, obtained by comparing snapshots of individual eyes at the beginning and end of a 1-hr period. N=10 at all points.

sampling method, so we adopted other approaches that allowed viewing of the entire eye. We immersed live embryos of ages 16–24 hpf for one hr in a solution of acridine orange (AO), a substance known to penetrate dying cells and concentrate in the nucleus (Abrams et al., 1993), and then viewed them a few minutes later, still alive, in a fluorescence microscope. Figure 2A shows one focal plane of such an eye and two AO+ nuclei, bright (yellow) spheres, are evident. They were generally well separated, as shown here, and so they were easily counted in a through-focus examination. Figure 3A gives these numbers as a function of age; they were always 1% or less of the total number of nuclei. All dying cells are believed to pass through this pyknotic state (Ellis et al., 1991), so it is considered to be a reliable "snapshot" of one phase of a process that generally lasts hours. We have also used the TUNEL method for detecting apoptotic cells and found comparably low numbers (unpublished results). Although these low numbers suggest that cell death was not quantitatively important, the number present at any time depends on how long they persist, and therefore snapshots of pyknotic cells cannot provide a basis for computing a rate of cell loss.

We were able to overcome this limitation when we discovered that we could recognize a dying cell even without AO staining. Eyes freshly exposed to AO were examined with fluorescence and/or differential interference contrast (DIC) optics. All AO+ nuclei were small, globular, and refractile relative to the other (AO-) nuclei, and all small, globular, and refractile nuclei were also AO+. This globular/refractile appearance (Fig. 2B) has previously been used to identify dying cells in *C. elegans*, another famously transparent

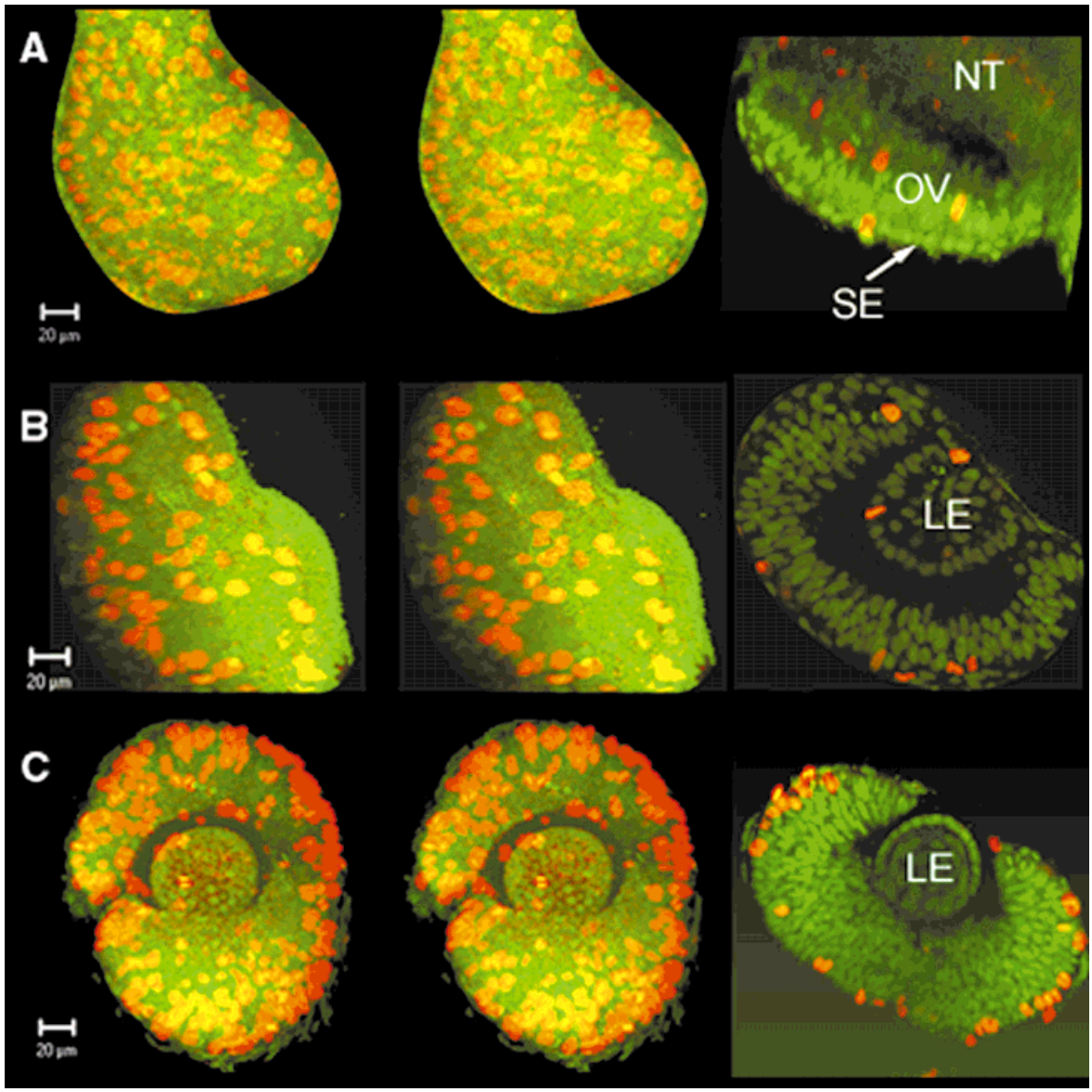

Fig. 4. Variation in the number of mitotic cells as a function of age. Mitotic cells are red (anti-phosphohistone H3) against a green nuclear stain (SYTO-13). The left two panels in each row form a stereo pair of an optic vesicle/eye, and the right panel is an optical section through this same structure. **A**: 14 hpf. The optic vesicle is flat and mitotic figures are numerous. **B**: 20 hpf. The eye cup has formed, and the mitotic figures are few. **C**: 36 hpf. The eye has matured, and the mitotic figures are numerous. LE, lens; NT, neural tube; OV, optic vesicle; SE, surface ectoderm.

embryo (Sulston and Horvitz, 1977). Rates of cell death were obtained directly, as follows. Several embryos were mounted for viewing in agarose after being lightly anesthetized to insure that they would remain still for an hour. Each was examined with DIC optics in a through-focus series, and all the pyknotic nuclei in one or both eyes were drawn through the drawing tube, with an annotation giving the depth (obtained from the indication on the fine focus knob of the microscope). The embryos were returned to the incubator, still in their viewing chambers, and an hour later they were viewed again and the pyknotic nuclei were drawn on the same sketch in a different color. Three classes of entries were scored: those that were present at both observations, those that were present at the first but absent from the second, and those that were absent from the first but present at the second. Figure 3B shows these data, which give a direct sampled measure of the rate of appearance and disappearance of pyknotic cells. The numbers of pyknotic cells detected at any time (Total) were similar to those estimated from the AO staining (Fig. 3A) and remained low until 36 hpf. The mean rates of appearance of new pyknotic cells (Added/hr) and disappearance of old ones (Lost/hr)

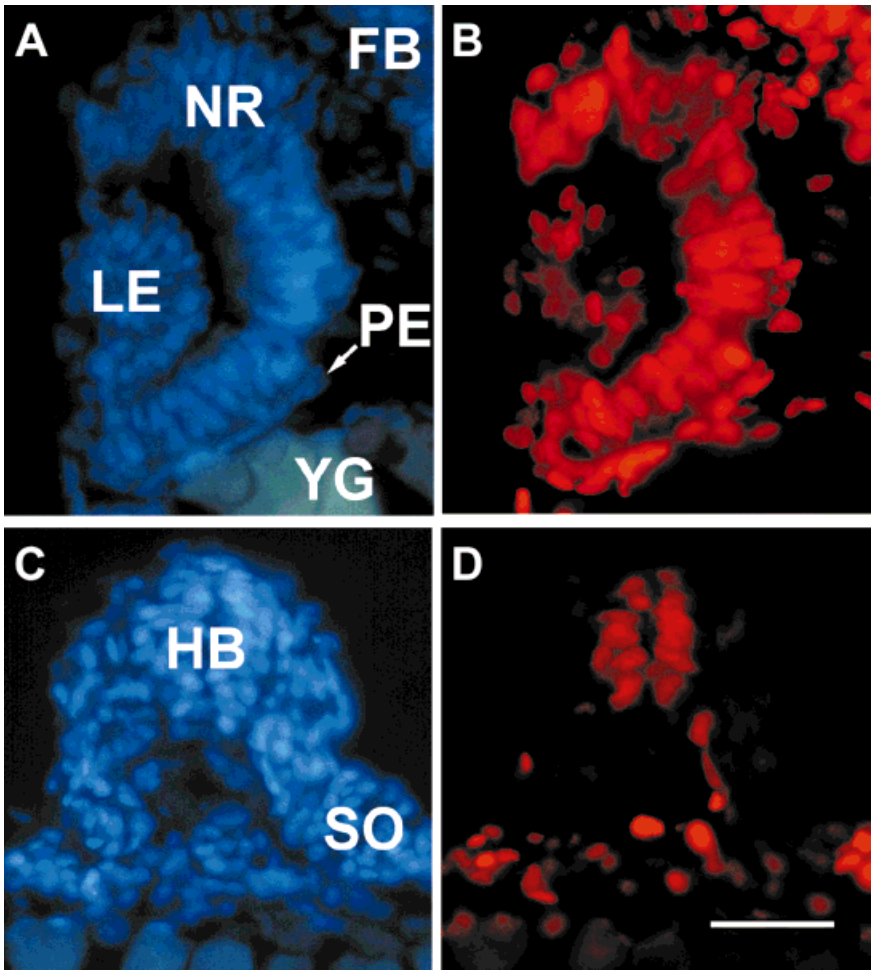

Fig. 5. Evidence that the reduced mitotic activity (Fig. 4B) is not a result of cells having withdrawn from the mitotic cycle. Fluorescence photomicrographs of transverse sections from a 22 hpf embryo that was injected with BrdU at 17 hpf. Nuclei stained red for BrdU (B, D) or with a blue nuclear stain (DAPI) (A, C). **A, B**: Eye. Nearly all the cells in the neural retina (NR) are BrdU+. **C, D**: Trunk. This is included to show the selectivity of the staining. The hindbrain (HB) is BrdU+, while the lateral somites (SO) are completely BrdU-. FB, forebrain; LE, lens; PE, pigmented epithelium; YG, yolk granules. Scale bar = 50 μm.

over the period 16–27 hpf are around 5/hr. At this rate, only about 55 cells would be lost over the 16–27 hpf interval, about 20× less than the 1114 that were predicted to have disappeared to balance the proliferation by a fully proliferative population with a T_C of 10 hr. Therefore cell death did not contribute importantly to the near constancy of cell number, and the rate of proliferation must have been considerably less than predicted. The next section shows how much less.

Modulated Proliferation

Age-related differences in mitotic activity were revealed by staining whole eyes with an antibody against the H3 phosphohistone. Figure 4 shows images from three eyes of different ages labeled in this way, the mitotic nuclei in red against a green nuclear stain. The two panels on the left of each row form a stereo pair and show that the density and absolute number of mitotic nuclei were considerably higher at 14 and 36 hpf than at the intermediate age of 20 hpf. The right panels show that the bulk of the mitotic figures were at the border of the optic lumen, adjacent to the ML/PE, as expected. Although we did not examine the neural tube in detail, our impression was that the mitotic activity there was more uniform over time, suggesting that these changes in proliferation were eye specific. The same sections that produced Figure 1A were scored for the percentage of cells in M-phase, and those data are shown in Figure 1B. The mitotic cells were only about 2–4% of the total over 16–24 hpf (compare Fig. 4B), and the percentage abruptly increased between 24 and 27 hpf to 10–12% and maintained that high value until 36 hpf (compare Fig. 4C). Concurrent with the increase in the fraction of mitotic cells, the cell number rose steeply, from 1406 ± 42 at 24 hpf to 3812 ± 184 at 36 hpf (Fig. 1A, B). This increase is

consistent with a doubling time of 8.3 hr or a T_C slightly shorter than that because some cells had quit the cell cycle. This value (hereafter approximated as 8 hr) is in reasonable agreement with 10 hr, the value previously reported for 24–28 hpf (Nawrocki, 1985). The images of Figure 4 and the numbers of Figure 1A, B indicate that proliferation decreased between 14–16 hpf and remained low until some time between 24–27 hpf, when it increased.

The rate of proliferation during 16–24 hpf was estimated from the data in Figure 1A, ignoring the small effects of cell death. During this 8-hr period, the number of cells increased from 1252 to 1406 (154 cells, or 12%), so the rate of proliferation averaged 1.5% per hr, which is only 21% of the rate (7% per hr) predicted on the basis of a completely proliferative cell population and a 10-hr T_C. The low rate could be caused by either a reduction of the proliferative fraction or an increase in T_C or both, and these two mechanisms are treated next.

A change in the proliferative fraction is considered first and rejected. For this mechanism to reduce proliferation to 21% of the expected value, 79% of the cells would have to withdraw from the mitotic cycle. To evaluate this possibility, we injected 5-bromo, 2-deoxyuridine (BrdU) into the yolk of 17 hpf embryos, sacrificed them after a survival of 5 hr, and then examined the eyes for BrdU-positive nuclei. The survival period spanned most of the interval when proliferation was reduced, and if most cells had withdrawn from the mitotic cycle then they should not have been labeled. The vast majority of nuclei were labeled (Fig. 5A, B), consistent with earlier reports that the proliferative fraction was 100% at this age (Nawrocki, 1985; Hu and Easter, 1999). This excludes the hypothesis that the proliferative fraction had been reduced and implies that T_C must have lengthened.

T_C was estimated independently in two ways and judged to be 4–6× longer during 16–24 hpf than during 24–36 hpf. The first estimate came from the change in total cell number. If the cycles of individual cells are assumed to be phased randomly, then an hourly increase of 1.5% corresponds to a T_C of 49 hr. T_C after 24 hpf has been estimated as either 10 hr (Nawrocki, 1985) or 8 hr (the present report), so T_C during 16–24 hpf was 5–6× longer than after 24 hpf. The second estimate came from a comparison of the fractions of cells in M-phase, with the assumptions that phases of all cells in the population are random and that the duration of M-phase (T_M) was the same at both ages (Quastler and Sherman, 1959). The fraction of cells in M-phase is equal to the ratio:

$$T_M/T_C.$$

After 24 hpf, when T_C was 8–10 hr, the fraction of mitotic cells was 10–12% (Fig. 1B), roughly 4× the 2–4% of M-phase cells during 16–24 hpf, which implies that T_C was about 4× greater, or about 32–40 hr, during 16–24 hpf. Thus, these two independent methods suggest that T_C was transiently prolonged to about 32–49 hr at about 16 hpf or earlier, and that this sluggish advance through the cell cycle persisted until some time between 24–27 hpf, when the advance speeded up (=T_C abruptly shortened to 8–10 hr) and remained at that value until at least 36 hpf, the oldest age considered here. This terminology is somewhat misleading because none of the cells could actually have had an intermitotic period of 32–49 hr. To say that cells transiently have a T_C of 49 hr is a statement of the rate of progress through the cell cycle; i.e., 1/49 of a cell cycle per hr.

The phase of the cell cycle most responsible for the deceleration appears to be S-phase. Following an injection with BrdU, the time needed to label all nuclei is the time needed to label those nuclei that had exited S-phase just prior to the injection, and this is the sum of the durations of G_2, M-phase, and G_1. Recall that the injection of BrdU described above labeled nearly all nuclei within 5 hr, which implies that S-phase must have occupied the remainder of T_C; this could have been as small as 32-5 = 27 or as large as 49-5 = 44 hr. In contrast, S-phase after 24 hpf was estimated to be about 7 hr (Nawrocki, 1985). Thus, the rate of DNA synthesis in the eye must have been greatly reduced during 16–24 hpf.

To learn if any other phases were decelerated, we used the "labeled mitotic figures" experimental paradigm (Quastler and Sherman, 1959) to examine G_2 and M-phases. Embryos of four ages (15, 19.5, 22.5, and 27 hpf) were injected with BrdU, survived 1 hr, and were stained like those in Figure 5. Interphase nuclei were ignored; only mitotic figures were scored as BrdU+ or BrdU-. All nuclei that were BrdU+ must have been in S-phase at or after the time of injection, and BrdU+ mitotic figures had progressed during the 1-hr survival through G_2 to M-phase. BrdU- mitotic figures identify those nuclei that had been in G_2 or M-phase at the time of injection. If G_2 were longer than 1 hr, all the mitotic figures in this experiment would remain BrdU-. Figure 6 shows that they did not; at all ages a fraction of the mitotic figures were labeled within 1 hr, which indicates that G_2 lasted less than 1 hr at all ages examined here. But the fraction of labeled mitotic figures was lower at the two intermediate ages than at the earliest and latest ages. This could have resulted from a larger denominator, i.e., an increase in the total number of mitotic figures, but Figure 1B shows that the total number of mitotic figures was essentially constant during 16–24 hpf, so this explanation is excluded. The dip in Figure 6 reflects a smaller numerator; that is, fewer nuclei progressed from S- to M-phase during the 1 hr following the injection, consistent with a prolongation of G_2 or M-phase or both. The major conclusions from the labeled mitotic figures experiment are first, that the advance through the cell cycle slowed down, but did not stop, at the two intermediate ages; second, that the

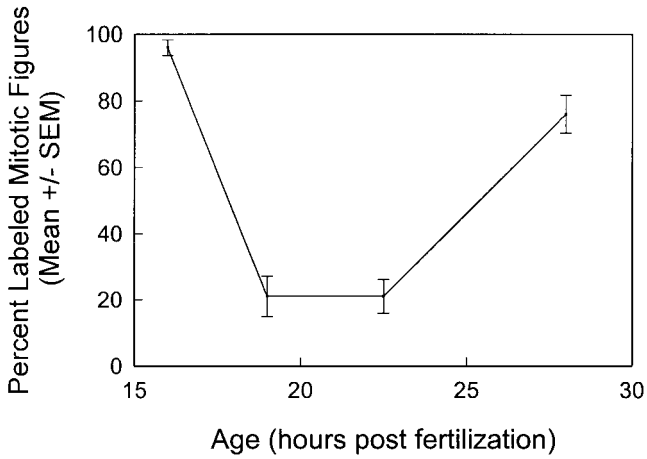

Fig. 6. Percent labeled mitotic figures as a function of age. Means ± SEM. Embryos of four ages were injected with BrdU and sacrificed 1 hr later, at the age shown on the abscissa. The ordinate shows the percentage of the mitotic figures that were BrdU+ at the time of sacrifice. This is a measure of speed of progress from S- to M-phase, and the dip at the two intermediate ages indicates that the speed had slowed.

advance began to slow after 15 hpf and sped up before 27 hpf; and third, that G_2 and possibly M-phase were prolonged, but probably did not contribute importantly to the lengthening of T_C, which measured in the 10s of hours.

Conclusions

The major conclusions of this article are summarized in Figure 7. Briefly, the number of cells in the developing eye increased very slowly during the pre-neurogenic morphogenesis of the eye cup and increased rapidly thereafter when neurogenesis began. Proliferation was reduced not by a diminution of the proliferative fraction, but by slowing the advance through the cell cycle (equivalent to increasing T_C) in all cells. When the advance accelerated, so did proliferation. Most of the slowing was in S-phase. Cell death was negligible throughout the time examined.

DISCUSSION

Modulation Vs. Monotonic Increase of T_C

Numerous studies of embryos, including zebrafish (Kane and Kimmel, 1993; Kimmel et al., 1994) have concluded that T_C is initially short, increases abruptly at the midblastula transition, and increases more gradually thereafter during gastrulation and organogenesis. Previous determinations of T_C in the vertebrate CNS have also described a steady lengthening with age (NR: Alexiades and Cepko, 1996; cerebral cortex reviewed by Caviness et al., 2000; neural tube reviewed by Jacobson, 1991). In zebrafish, the ocular T_C prior to 16 hpf has not been determined, but in the spinal cord, T_C is 5–8 hr at 15–20 hpf (Kimmel et al., 1994), so we assume that the ocular T_C was probably 9 hr or less prior to 16 hpf. We have shown that it lengthened to 32–49 hr between 16–24 hpf, and then abruptly shortened thereafter to 8–10 hr. These abrupt changes are unusual, and the shortening around 24 hpf is an exception to the general rule that T_C increases monotonically. We emphasize that the long values of T_C (32–49 hr) were experienced only transiently, and indicate a decelerated rate of progress through the cell cycle, not intermitotic intervals.

In *Drosophila*, modulation of T_C is widespread and important to development. In the imaginal disks, T_C lengthens because the progress through the cycle arrests for hours in G_2 (Fain and Stevens, 1982; Graves and Schubiger, 1982) or G_1 (Thomas et al., 1994) and then shortens as the cell advances to the next phase of the cycle. Such arrests have the effect of synchronizing local populations of cells, a phenomenon best seen in the vicinity of the morphogenetic furrow in the eye imaginal disk (reviewed by Thomas and Zipursky, 1994). When synchronization is genetically perturbed during neurogenesis, the ommatidial pattern is abnormal (Penton et al., 1997), suggesting that synchronization is important to patterning. This importance may be related to the cell cycle phase-specific expression of certain genes; e.g., those for receptors which must appear when their ligand is present (McConnell and Kaznowski, 1991; Urdiales et al., 1998). These results contrast sharply with those of Harris and Hartenstein (1991), who found that the differentiation of retinal neurons proceeded grossly normally in the absence of *any* cell division over a period when three divisions would normally have occurred. If differentiation can proceed in the absence of cell division, one is tempted to doubt that any developmental function can be served by modulation or synchronization of T_C. We resist this temptation because of the results mentioned earlier in this paragraph and because of our recent demonstration that early neurogenesis in the zebrafish NR follows an intricate spatiotemporal program in which particular neurons are produced by terminal mitotic divisions at stereotyped times and places (Hu and Easter, 1999). These observations indicate that the cell cycle is under closer control in vertebrate development than had previously been thought.

The increase in T_C that we have shown in the zebrafish eye is mechanistically quite different from what occurs in the fly imaginal disks. The demonstration that most cells incorporated BrdU during 17–22 hpf (Fig. 5) argues against a G_2 arrest, but it is conceivable that all those nuclei that labeled early completed their S-phase and then arrested in G_2. This possibility is unlikely because arrest at G_2 means that no mitotic figures would form, but as Figure 1B summarizes, they were observed throughout 16–24 hpf, suggesting that the advance from G_2 to M-phase was normal. But this observation alone is not completely convincing, because if the nuclei in M-phase at 16 hpf had arrested, they would have persisted throughout 16–24 hpf, consistent with Figure 1B. This explanation (G_2 and M-phase arrests) can be excluded by the labeled mitotic figures

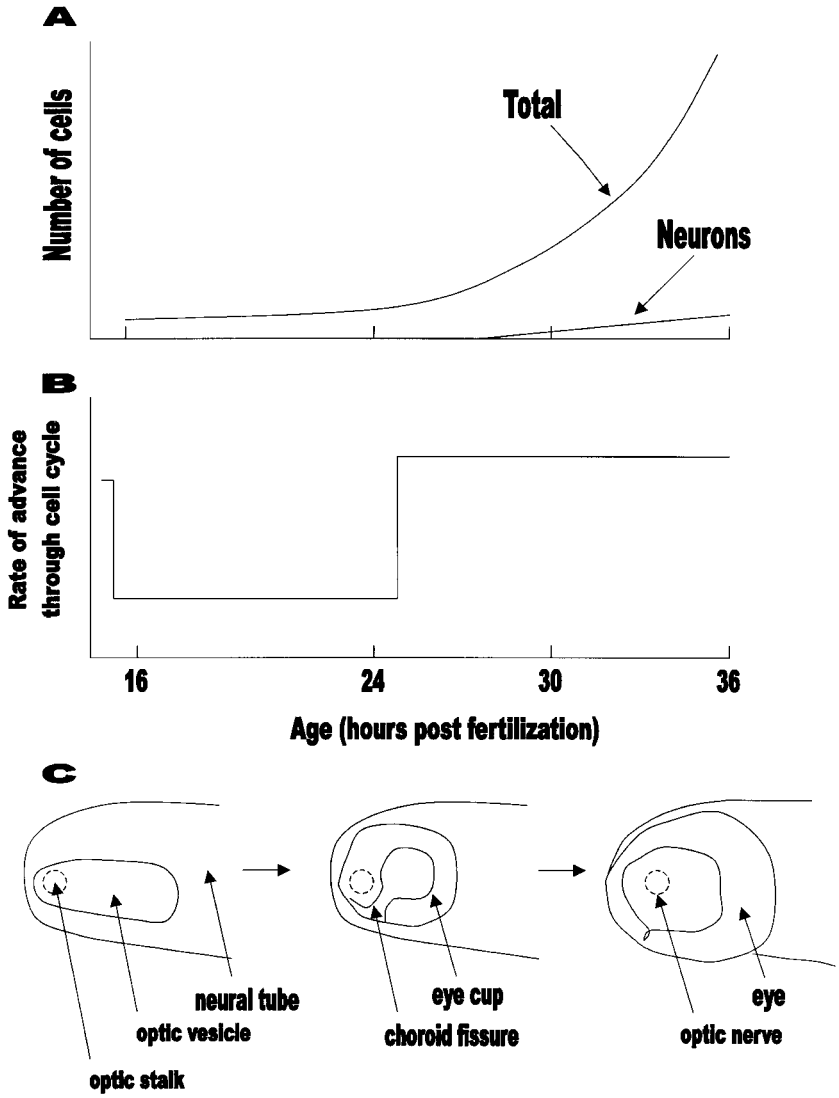

Fig. 7. Summary of results, incorporating information from Hu and Easter (1999), Li et al. (2000), and Schmitt and Dowling (1994). **A**: The number of cells in the developing eye vs. age. The number rose sluggishly during the pre-neurogenic period of eye cup morphogenesis and then explosively when neurogenesis began. The numbers of neurons remained a small fraction of the total number of cells, and all the neurons were of the same type, ganglion cells (Hu and Easter, 1999). **B**: The rate of advance through the cell cycle (the inverse of T_C) vs. age. The rate abruptly slowed prior to 16 hpf and accelerated between 24 and 27 hpf and remained high until 36 hpf. **C**: Sketches of lateral views of embryos (dorsal up, anterior left), illustrating the transformation of the flat optic vesicle (16 hpf) into the spherical eye cup with an open choroid fissure (24 hpf), and finally into the eye with a fused choroid fissure and optic nerve fibers in the stalk (36 hpf).

experiment (Fig. 6) which showed that nuclei progressed from S-phase to M-phase, and from M-phase to G_1 during this period, excluding any widespread arrest. Therefore the cells in the zebrafish eye did not arrest at either M-phase or G_2 during 16–24 hpf. Nor could they be said to have arrested in S-phase; the term "S-phase arrest" is usually used to indicate a state of interrupted DNA synthesis before completion (Smerdely et al., 1993). Instead of arresting, the cells decelerated the advance through G_2, M-, and S-phases. The prolonged S-phase is consistent with other reports of prolonged T_C from the NR (Alexiades and Cepko, 1996) and cortex (Gressens et al., 1998). The mechanism of prolongation is unknown, but two possibilities exist and both involve the replicons, the segments of chromosomal DNA that are replicated as units and then joined together. The time over which the replicons are initiated may be lengthened, and/or the number of replicons may be decreased, which increases the size of the replicons (Blumenthal et al., 1974; McKnight and Miller, 1977; Walter and Newport, 1997).

In view of the fact that T_C was modulated during the morphogenesis of the eye, it is instructive to examine neurulation, another well studied case of morphogene-

sis, to see if T_C is modulated in ways that might suggest a function in the eye. Smith and Schoenwolf (1988) found regional rather than temporal modulation of T_C and they constructed an interesting argument. The cells in the hinge points (the regions around which the neural plate bends) have a longer T_C than the adjacent cells. This would impart a structural advantage, as wedge-shaped cells in this region, short in the apicobasal direction with a broad basal end and a narrow apical one, are conducive to the bending of the adjacent neural plate. The broadest part of a columnar epithelial cell is where its nucleus is, and the nuclear location is set by the phase of the cell cycle. If some phase of the cell cycle other than M-phase is prolonged, the nucleus remains in the basal end, which promotes the bending of the neural plate. While this explanation works well for the neural plate, it does not transfer well to our results because of the different topology of the optic vesicle and the neuroectoderm. In the optic vesicle, the basal surface of the NR is concave, whereas in the dorsal neuroectoderm the basal surface is convex. For this reason, the transformation from flat vesicle to curved eye cup would be facilitated if nuclei were at their apical positions (adjacent to the ML/PE) but this is the location occupied by mitotic cells, which are in short supply at the time the curvature develops (Fig. 4B).

We have no satisfactory suggestion for why a lengthened T_C during morphogenesis might be adaptive. During the course of the cell cycle, proliferating cells release their basal endfeet from the inner limiting membrane and expand their area on the outer limiting membrane, then release space there and reclaim space on the inner limiting membrane. Such acrobatics might interfere with the movements of sheets of cells parallel to the limiting membranes, and if they did, then suppression of the cell cycle would be adaptive. This suggestion leads to the prediction that proliferation may be suppressed generally in those epithelial sheets involved in complex shape changes, such as the formation of placodal vesicles, but to our knowledge this issue has not been examined. As for a "proximate" cause of the lengthening, we note that proliferation appears to slow down and then to speed up simultaneously all over the retina, consistent with control by widely diffusible factors rather than a cascade of cell-to-cell contacts.

Cell Death

We have recognized dying cells in vivo by the appearance of their nuclei. Visualization in vivo allows an examination of dying cells over time, without which the rate of loss cannot be known. This approach has an advantage over histological methods which involve sections of dead tissue and therefore provide a view of only one time. Direct visualization of dying cells in vivo is not possible in most embryos, and in them the rate of loss must be estimated from snapshots of dying cells. This requires knowing the clearance time, defined as the interval over which a dying cell is recognizable as such prior to its disappearance. Estimates of clearance time generally depend on uncertain assumptions and range widely, e.g., from 40 min (Voyvodic et al., 1995) to 3 hr (Harvey and Robertson, 1992) in rat NR (but see Thomaidou et al., 1997, for an ingenious method that makes these assumptions unnecessary). With a transparent embryo we were able to obtain the rate of loss directly. The rates that we measured did not depend on knowing the clearance time, but we can estimate it from our results. Around 16 hpf, the total number of pyknotic cells was about 15 and the hourly rate of loss was about 5. Surprisingly, the same ratios obtained at 38 hpf, when the total was about 6 and the hourly rate of loss was about 2. That is, over an hour about a third of the dying cells disappeared, which means that the clearance time was about 3 hr.

The surprisingly small amount of cell death is consistent with other studies of the embryonic and larval retinas of fish (Daly and Sandell, 2000; Hoke and Fernald, 1998) and frogs (Gaze and Grant, 1992). The observations have also been extended to adult fish retinas, in which continuous growth produces a chronotopic pattern with old cells in the center and progressively younger cells more peripheral, so all phases of retinal development are visible in a section through the center of the eye. Yet Hoke and Fernald (1998) found no elevated concentration of TUNEL+ cells anywhere, which suggests that fish retinas never experience a significant cell death. Gaze and Grant (1992) used a different approach to estimate cell death in the *Xenopus* retina; they counted the number of ganglion cells in corresponding regions of young and old retinas and found a significant drop around the time of metamorphosis. Both the magnitude and the timing of the loss are different in frogs vs. mammals, especially rat, in which ganglion cells begin to die almost as soon as they are born and 90% of those born ultimately die (Galli-Resta and Ensini, 1996). The retinas of anamniotes show a greater delay and a lesser loss, and in the case of fish, perhaps no loss at all.

The Strength of Numbers

All of our conclusions depended on our knowledge of the numbers of cells, living, dying, and mitotic. The standard criteria for concluding that a tissue is proliferative are the presence of mitotic figures and the ability to be labeled with BrdU, but neither of these can provide an estimate of the rate of proliferation. Only the counts could provide that information, and they led directly to the major conclusions: The LL/NR acquired hundreds of cells from the ML/PE by intraocular cellular rearrangement, cell death was negligible, and T_C was modulated up and down.

EXPERIMENTAL PROCEDURES

Embryos

Adult zebrafish were maintained in our own facility in 10 gallon aquaria with a controlled light cycle of 14

hr light / 10 hr dark at 28.5°C. They spawned soon after the onset of light, and the fertilized eggs were collected approximately 2 hr after the lights came on. Embryos with the same number of cells (range 2–8) were sorted into individual petri dishes containing embryo rearing solution (ERS: 0.004% $CaCl_2$, 0.0163% $MgSO_4$, 0.1% NaCl, and 0.003% KCl), and the dishes were labeled with the number of cells and the time of sorting and kept in an incubator at 28.5°C. The first division occurs at 0.75 hpf and the next three divisions occur at 0.25 hr intervals thereafter (Kimmel et al., 1995), so the exact time of fertilization was estimated by the cell number at the time of sorting.

Cell Counts

Individual embryos (16, 18, 20, 24, 27, 30, 33, and 36hpf) were fixed in a mixture of 2% glutaraldehyde and 2% paraformaldehyde in 100 mM phosphate buffer, pH 7.4, rinsed, dehydrated in a graded series of ethyl alcohols, cleared in propylene oxide, and embedded in Epon. Sections (1 or 2 μm thick) were cut on an ultramicrotome (Ultracut, American Optical), stained with toluidine blue, and coverslipped. They were cut in groups of 10 sections and mounted on microscope slides with teflon-isolated wells: The first seven were kept together in one well, and the eighth, ninth, and tenth were isolated, in order, in the next three individual wells for analysis with the assumption-free optical disector method of nuclear tops (Coggeshall, 1992; Coggeshall and Lekan, 1996). Two of the three serial sections were drawn in a *camera lucida* to show all nuclear fragments, including interphase, mitotic, and pyknotic. These drawings were then superimposed on one another, and those nuclear fragments in one section that were not represented in the other were, by definition, "nuclear tops." Tops were counted at 6–10 sites separated by 10 μm (the number of sites depended on the size of the eye and the plane of section). At each site, the eighth and tenth sections were superimposed. The number of nuclei in the entire eye was computed by multiplying the total number of counted tops by the ratio:

$$\frac{\text{(distance between sample sites)}}{\text{(distance between sampled sections)}}.$$

The numerator was always 10, but the denominator was either 2 or 4 according to whether the sections were 1 μm or 2 μm thick, respectively.

Cell Death

Dying cells were detected by the presence of pyknotic nuclei in both sections and intact live eyes. In sections they were recognized by their small size and intense toluidine blue stain, a standard terminal marker of dying cells (Kerr et al. 1995). In live eyes they were detected by two criteria: AO staining (Abrams et al., 1993) and unstained nuclear anatomy. Embryos were dechorionated, soaked for 1 hr in ERS containing 1% AO, removed, rinsed several times in fresh ERS, and then mounted in low melting point agarose in a shallow well on a microscope slide and coverslipped. They were observed through a long working distance water-immersion objective (50×) on a compound microscope (Aristaplan, Leitz) equipped with fluorescence and DIC optics. AO penetrates the membranes of dead cells and concentrates in their nuclei, where it is revealed in a fluorescence microscope with a fluorescein cube. A through-focus examination of the eye revealed the AO+ nuclei, which were counted directly. Examination of the same embryos with DIC but without fluorescence revealed that the AO+ nuclei had a distinct globular shape and a highly refractile interior that allowed their detection even without the AO.

Mitotic Cells

Mitotic cells were recognized in semithin sections by the toluidine-blue-stained condensed chromatin which was darker than interphase nuclei. We also used an antibody against phosphohistone H3 (06-570, Upstate Biotechnology) on whole-mounted eyes. Embryos were fixed in 100 mM phosphate-buffered 4% paraformaldehyde, rinsed in buffer, permeabilized by soaking 20–30 min in 100 mM phosphate buffered 0.1% collagenase (C-2139, Sigma), and partially slit along the dorsal midline to allow access to the eyes from both sides. Whole animals were incubated in the primary antibody overnight on a shaker table, rinsed, and incubated overnight with a secondary antibody coupled to Cy-3 (red) (711-165-152, Jackson ImmunoResearch Laboratories). They were counterstained 6–10 minutes with a fluorescent green nuclear stain (SYTO 13, Molecular Probes), cleared in 70% glycerol/30% fix, and the eyes were either dissected free and mounted alone or the whole embryo was mounted, dorsal side up, in a shallow well on a microscope slide. They were viewed in a laser scanning confocal microscope (LSM 510, Zeiss).

BrdU Labeling

S-phase cells were labeled with BrdU as described elsewhere (Hu and Easter, 1999). Briefly, yolk sacs of individual embryos were pressure-injected with approximately 0.5 nl of an aqueous solution of 10 mM BrdU (B-5002, Sigma). Following a survival of 1 or 4 hr, depending on the experiment, they were fixed in 100 mM phosphate-buffered 4% paraformaldehyde, and frozen-sectioned at 10 μm. The sections were permeabilized on the slide, exposed to 2N HCl to denature the DNA, blocked with 100 mM lysine in 100 mM phosphate buffer, and incubated with an anti-BrdU monoclonal antibody (MAS-250, Harlan). Incubation with a red fluorescent secondary antibody (712-165-153, Jackson ImmunoResarch Laboratories) followed, and the sections were counterstained with DAPI prior to being mounted (Anti-Fade, Molecular Probes) and coverslipped.

REFERENCES

Abrams JM, White K, Fessler LI, Steller H. 1993. Programmed cell death during *Drosophila* embryogenesis. Development 117:29–43.

Alexiades MR, Cepko C. 1996. Quantitative analysis of proliferation and cell cycle length during development of the rat retina. Dev Dyn 205:293–307.

Burnside MB, Jacobson AG. 1968. Analysis of morphogenetic movements in the neural plate of the newt *Taricha torosa*. Dev Biol 18:537–552.

Blumenthal AF, Kriegstein HJ, Hogness DS. 1974. The units of DNA replication in Drosophila melanogaster chromosomes. Cold Spring Harb Symp Quant Biol 38:205–223.

Burt AS. 1943. Neurulation in mechanically and chemically inhibited Amblystoma. Biol Bull 85:103–115.

Caviness VS Jr, Takahashi T, Nowakowski RS. 2000. Neuronogenesis and the early events of neocortical histogenesis. In: Goffinet M, and Rakic P, editors. Mouse brain development. Berlin: Springer-Verlag. (in press)

Coggeshall RE. 1992. A consideration of neural counting methods. Trends Neurosci 15:9–13.

Coggeshall RE, Lekan HA. 1996. Methods for determining numbers of cells and synapses: a case for more uniform standards of review. J Comp Neurol 364:6–15.

Daly FJ, Sandell JH. 2000. Inherited retinal degeneration and apoptosis in mutant zebrafish. Anat Rec 258:145–155.

Ellis RE, Yuan JY, Horvitz HR. 1991. Mechanisms and functions of cell death. Annu Rev Cell Biol 7:663–698.

Fain MJ, Stevens B. 1982. Alterations in the cell cycle of *Drosophila* imaginal disc cells precede metamorphosis. Dev Biol 92:247–258.

Galli-Resta L, Ensini M. 1992. An intrinsic time limit between genesis and death of individual neurons in the developing retinal ganglion cell layer. J Neurosci 16:2318–2324.

Gaze RM, Grant P. 1992. Spatio-temporal patterns of retinal ganglion cell death during *Xenopus* development. J Comp Neurol 315:264–274.

Gillette R. 1944. Cell number and cell size in the ectoderm during neurulation (*Amblystoma maculatum*). J Exp Zool 96:201–222.

Graves BJ, Schubiger G. 1982. Cell cycle changes during growth and differentiation of imaginal leg discs in *Drosophila melanogaster*. Dev Biol 93:104–110.

Gressens P, Paindaveine B, Hill JM, Evrard P, Brenneman DE. 1998. Vasoactive intestinal peptide shortens both G1 and S phases of neural cell cycle in whole postimplantation cultured mouse embryos. Eur J Neurosci 10:1734–1742.

Harris WA, Hartenstein V. 1991. Neuronal determination without cell division in Xenopus embryos. Neuron 6:499–515.

Harvey AR, Robertson D. 1992. Time-course and extent of retinal ganglion cell death following ablation of the superior colliculus in neonatal rats. J Comp Neurol 325:83–94.

Hoke KL, Fernald RD. 1998. Cell death precedes rod neurogenesis in embryonic teleost retinal development. Dev Brain Res 111:143–146.

Holt C. 1980. Cell movements in *Xenopus* eye development. Nature 287:850–852.

Hu M, Easter SS Jr. 1999. Retinal neurogenesis: the formation of the initial central patch of postmitotic cells. Dev Biol 207:309–321.

Jacobson, M. 1991. Developmental Neurobiology (3rd edition) New York: Plenum Press.

Kane DA, Kimmel CB. 1993. The zebrafish midblastula transition. Development 119:447–456.

Kerr JFR, Gobe' GC, Winterford CM, Harmon BV. 1995. Anatomical methods in cell death. Methods Cell Biol 46:1–27.

Kimmel CB, Warga RM, Kane DA. 1994. Cell cycles and clonal strings during formation of the zebrafish central nervous system. Development 120:265–276.

Kimmel CB, Ballard WW, Kimmel SR, Ullmann B, Schilling TF. 1995. Stages of embryonic development of the zebrafish. Dev Dyn 203: 253–310.

Li Z, Easter SS Jr. 1997. The development of eye in the zebrafish embryo. Abstr Soc Neurosci 23:1966.

Li Z, Joseph NM, Easter SS Jr. 2000. The morphogenesis of the zebrafish eye, including a fate map of the optic vesicle. Dev Dyn 218:175–188.

Marcus RC, Delaney CL, Easter SS Jr. 1999. Neurogenesis in the visual system of embryonic and adult zebrafish (*Danio rerio*). Vis Neurosci 16:417–424.

McConnell SK, Kaznowski CE. 1991. Cell cycle dependence of laminar determination in developing neocortex. Science 254:282–285.

McKnight SL, Miller OL. 1977. Electron microscopic analysis of chromatin replication in the cellular blastoderm Drosophila melanogaster embryo. Cell 12:795–804.

Nawrocki L. 1985. Development of the neural retina in the zebrafish, *Brachydanio rerio*. PhD thesis. University of Oregon, Eugene.

Penton A, Selleck SB, Hoffmann FM. 1997. Regulation of cell cycle synchronization by *decapentaplegic* during *Drosophila* eye development. Science 275:203–206.

Oppenheim RW 1991. Cell death during development of the nervous system. Annu Rev Neurosci 14:453–502.

Quastler H, Sherman FG. 1959. Cell population kinetics in the intestinal epithelium of the mouse. Exp Cell Res 17:420–438.

Schmitt EA., Dowling JE. 1994. Early eye morphogenesis in the zebrafish, *Brachydanio rerio*. J Comp Neurol 344:532–542.

Smerdely P, Pitsiavas V, Boyages SC. 1993. Methimazole inhibits FRTL5 thyroid cell proliferation by inducing S-phase arrest of the cell cycle. Endocrinology 133:2403–2406.

Smith JL, Schoenwolf GC. 1988. Role of cell-cycle in regulating neuroepithelial cell shape during bending of the chick neural plate. Cell Tissue Res 252:491–500.

Sulston JE, Horvitz HR. 1977. Post-embryonic cell lineages of the nematode, *Caenorhabditis elegans.* Dev Biol 56:110–156.

Thomaidou D, Mione MC, Cavanagh JFR, Parnavelas JG. 1997. Apoptosis and its relation to the cell cycle in the developing cerebral cortex. J Neurosci 17:1075–1085.

Thomas BJ, Zipursky SL. 1994. Early pattern formation in the developing *Drosophila* eye. Trends Cell Biol 4:389–394.

Thomas BJ, Gunning DA, Cho J, Zipursky SL. 1994. Cell cycle progression in the developing *Drosophila* eye: *roughex* encodes a novel protein required for the establishment of G1. Cell 77:1003–1014.

Urdiales JL, Becker E, Andrieu M, et al. 1998. Cell cycle phase-specific surface expression of Nerve Growth Factor receptors TrkA and $p75^{NTR}$. J Neurosci 18:6767–6775.

Voyvodic JT, Burne JF, Raff MC. 1995. Quantification of normal cell death in the rat retina: implications for clone composition in cell lineage analysis. Eur J Neurosci 7:2469–2478.

Walter J, Newport JW. 1997. Regulation of replicon size in *Xenopus* egg extracts. Science 275:993–995.